THE JOURNAL OF PHYSICAL CHEMISTRY B

Article

pubs.acs.org/JPCB

Dynamics in the Isotropic Phase of Nematogens Using 2D IR Vibrational Echo Measurements on Natural-Abundance ^{13}CN and Extended Lifetime Probes

Kathleen P. Sokolowsky and Michael D. Fayer*

Department of Chemistry, Stanford University, Stanford, California 94305, United States

Supporting Information

ABSTRACT: The long time scale orientational relaxation of nematogens in the isotropic phase is associated with the randomization of pseudonematic domains, which have a correlation length that grows as the isotropic-to-nematic phase transition temperature is approached from above. Here we begin to address the fast dynamics of the nematogen molecules within the domains using two-dimensional infrared (2D IR) vibrational echo experiments. The problems of performing ultrafast IR experiments in pure liquids are discussed, and solutions are presented. In addition, the issue of short vibrational lifetimes, which limit the ability of 2D IR experiments to examine dynamics over a wide range of times, is addressed. The experiments were performed on the nematogen 4-cyano-4′-pentylbiphenyl (5CB), with the CN stretch initially used as the vibrational probe. Although the CN stretch has a small transition dipole, because the sample is a pure liquid it is necessary to use an exceedingly thin sample to perform the experiments. The small sample volume leads to massive heating effects that distort the results. In addition, the high concentration in the pure liquid can result in vibrational excitation transfer that interferes with the measurements of structural dynamics, and the CN vibrational lifetime is very short (3.6 ps). These problems were overcome by performing the experiments on the natural-abundance ^{13}CN stretch (5^{13}CB), which greatly reduced the absorbance, eliminating the heating problems; also, this stretch has a longer lifetime (7.9 ps). Experiments were also performed on benzonitrile, which showed that the heating problems associated with pure liquids are not unique to 5CB. Again, the problems were eliminated by conducting measurements on the ^{13}CN stretch, which has an even longer lifetime (20.2 ps) compared with the ^{12}CN stretch (5.6 ps). Finally, to extend the range of the dynamical measurements, 4-pentyl-4′-thiocyanobiphenyl (5SCB) was synthesized and studied as a dilute solute in 5CB. The CN stretch of 5SCB has a vibrational lifetime of 103 ps, which permits dynamical measurements to 200 ps, revealing the full range of fast structural dynamics in the isotropic phase of 5CB. It is shown that the 5SCB probe reports essentially the same dynamics as 5^{13}CB on the short time scale that is observable with the 5^{13}CB vibrational probe.

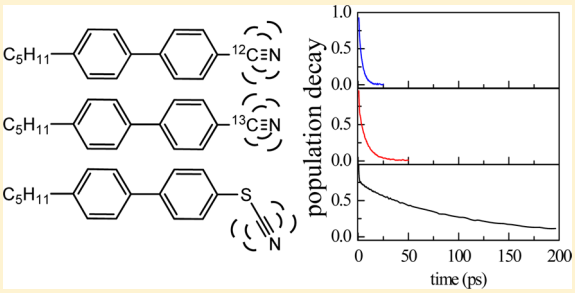

I. INTRODUCTION

The orientational relaxation dynamics of nematic liquid crystals in the isotropic phase differ greatly from that of traditional liquids. These relatively long time scale dynamics have been studied by a wide variety of time-[1−4] and frequency-domain[5−9] experiments, including optical Kerr effect spectroscopy in our lab.[10−14] At temperatures above the nematic−isotropic phase transition, the orientational relaxation dynamics are dominated by the randomization of pseudonematic domains characterized by a correlation length, ξ.[15] As the nematic−isotropic transition temperature is approached from above, ξ grows as described by Landau−de Gennes theory[15] until it becomes infinite in the nematic phase. The Landau−de Gennes theory accurately describes the temperature dependence of the final slow exponential orientational relaxation of the nematogens in the isotropic phase. However, Landau−de Gennes theory does not describe the nonexponential orientational relaxation that occurs on time scales that are short compared with the final exponential complete orientational relaxation. Orientational relaxation on both short and long time scales has been studied experimentally with optical heterodyne-detected optical Kerr effect (OHD-OKE) experiments[10,11,13,16] and with theory.[14] OHD-OKE experiments examine the collective orientational relaxation dynamics on all time scales but do not address the dynamics experienced by the individual nematogen molecules within the domains and the dynamics arising from the full range of molecular motions. To look at these dynamics, techniques other than OHD-OKE experiments need to be employed.

Two-dimensional infrared (2D IR) vibrational echo spectroscopy provides a means of extracting subpicosecond to >100 ps time scale structural dynamics through the measurement of spectral diffusion of a vibrational probe that is caused by the evolution of a medium's (liquid, protein, etc.) structure.[17−19] Ultrafast vibrational echo experiments have been applied to the

Received: July 19, 2013
Revised: October 24, 2013

   dx.doi.org/10.1021/jp4071955 | J. Phys. Chem. B XXXX, XXX, XXX−XXX

study of a broad range of condensed-phase systems, including the hydrogen-bonding network in water, the folding of small peptides, and the dynamics of a catalyst attached to a monolayer.[20−44]

The 4-cyano-4′-alkylbiphenyl (*n*CB) series of liquid crystals exhibit nematic phases for $n = 5-9$ and have been well-studied using a variety of techniques.[2,5−7,10,11,13,45−53] The first of these compounds to be synthesized, 4-cyano-4′-pentylbiphenyl (5CB), has a nematic−isotropic transition temperature of 35 °C.[47] To study a liquid crystal by 2D IR spectroscopy, it is necessary to have a vibrational probe that does not fundamentally alter the nature of the liquid crystal under study. The nitrile stretch of 5CB is a sharp peak around 2230 cm^{-1} and can act as a vibrational probe for 2D IR experiments.[5] Nitriles have previously been shown to be adequate vibrational probes, although they possess relatively small transition dipoles and short vibrational lifetimes.[23,24,27,54] However, using the CN stretch of 5CB results in significant problems that ultimately require a different approach.

To study the dynamics of the pseudonematic domains of 5CB, it is necessary to study 5CB as a pure liquid. Dissolution of 5CB in traditional solvents eliminates the fundamental liquid-crystal nature of 5CB and prevents the formation of the pseudonematic domains of interest. The high concentration of vibrational probes in pure liquids complicates ultrafast mid-IR experiments. Even for vibrational probes with weak transition dipoles, samples of pure liquids must be exceedingly thin so that the absorbance is not too great, a requirement for 2D IR vibration echo experiments to be performed. In limiting the optical density of the sample, the number of molecules excited by impinging laser pulses is also decreased. In studies of water, the hydroxyl stretch is used as the vibrational probe. To reduce the heating problem, generally dilute HOD is studied in either H_2O (using the OD stretch as the probe) or D_2O (using the OH stretch as the probe).[20,39,41,43,55−57] Even for isotopically dilute water studies, heating is still readily evident.[28,57] In water, heating shifts the equilibrium distribution of hydrogen bonds, which produces new absorptions and residual bleaches in 2D IR spectra and IR pump−probe spectra due to a shifted center of the hydroxyl stretch spectrum.[28] The new features last until thermal diffusion cools the laser-heated spot. Studies of HOD in H_2O or D_2O do not completely eliminate the heating problems, but water dynamics are so fast that it is possible to make meaningful measurements prior to the onset of the deleterious effects of vibrational-relaxation-generated heating.

Besides unintentional experimental heating, 2D IR experiments on pure liquids are more likely to be affected by vibrational excitation transfer.[58−60] Once again, the high concentration of vibrational probes places the excited species in close proximity to an unexcited identical species. As excitation transfer decays as the distance to the sixth power, pure liquids provide a prime environment for this phenomenon. Although there are no reports on vibrational excitation transfer in 5CB, multiple simulations suggest low-energy parallel and antiparallel conformations of dimers in the nematic phase.[61−63] Several of these configurations place nitrile groups on neighboring 5CB molecules at a distance of 0.5 to 1 nm.[63] Thus, it is possible that vibrational excitation transfer occurs in the pseudonematic domains of pure 5CB. In water, studying the OD stretch of dilute HOD in H_2O or the OH stretch of dilute HOD in D_2O eliminates the possibility of vibrational excitation transfer.

Here we address the problems encountered when performing ultrafast mid-IR experiments on 5CB as a pure liquid. As with pure water, drastic heating of the sample occurs, obscuring the underlying dynamics in the pseudonematic domains on all but the shortest times. Dynamics can only be extracted from the 2D IR spectra to ∼6 ps. Even then, the measurements are possibly contaminated by vibrational excitation transfer. We garner no valuable information from this short window other than the observation that the nitrile probe does not sample all possible environments. We solved the problems associated with examination of pure 5CB using 2D IR by conducting experiments on the natural-abundance ^{13}CN nitrile stretch of 5CB ($5^{13}CB$).

Analogous to pure water, the isotopic substitution of an atom in the vibrational probe of 5CB shifts the center frequency of the stretch. The combination of the frequency shift and the low concentration afforded by the 1.1% natural abundance of carbon-13 eliminates vibrational excitation transfer among the dilute $5^{13}CB$ molecules. More importantly, the low concentration of $5^{13}CB$ allows us to prepare samples that are ∼100 times thicker than in the studies of the ^{12}CN stretch ($5^{12}CB$). Temperature changes in the sample are decreased by the same magnitude; thus, 2D IR spectra are not contaminated by heating or vibrational excitation transfer. The measurements provide dynamical information to ∼30 ps, limited by the lifetime of the probe rather than the growth of heat-induced peaks. The vibrational lifetime of $5^{13}CB$ was found to be significantly longer than that of $5^{12}CB$, demonstrating that a different vibrational relaxation pathway occurs in the carbon-13 molecules compared with the carbon-12 molecules.[64,65]

We confirmed that the strategy of natural-abundance carbon-13 experiments is not a unique feature to 5CB through the study of benzonitrile. A thin sample of benzonitrile showed even more dramatic heating effects than 5CB, an issue that was solved by making the sample much thicker and probing the ^{13}CN stretch. Just as with 5CB, a vibrational lifetime increase was also observed for the ^{13}CN stretch versus the ^{12}CN stretch. This suggests the applicability of natural-abundance carbon-13 probes to other pure liquids containing a carbon in the vibrational label (CO, CH, etc.).

To further increase the time range of the 2D IR experiments, we synthesized 4-pentyl-4′-thiocyanobiphenyl (5SCB). We then conducted ultrafast mid-IR experiments on the CN stretch of dilute 5SCB as a solute in 5CB to increase the range of the dynamical measurements. It has been shown that the addition of a heavy "blocking" atom between a nitrile stretch and the remainder of a molecule substantially increases the lifetime of the vibration.[66−68] We found that 5SCB as a solute in 5CB has a vibrational lifetime of ∼100 ps. At short times, the CN stretch of 5SCB reports essentially the same dynamics as $5^{13}CB$. The long lifetime of the CN stretch of 5SCB allowed us to measure the full range of fast structural dynamics in the isotropic phase of 5CB at 329 K, limited only by our present ability to delay laser pulses to 200 ps. In subsequent work using OHD-OKE experiments, we will show that the introduction of a small amount of 5SCB does not significantly alter the pseudonematic domains, phase transition, and orientational dynamics 5CB. Therefore, 5SCB can serve as a useful probe of the dynamics of the isotropic phase of 5CB.

II. EXPERIMENTAL METHODS

A. Sample Preparation. 5CB was purchased from Sigma-Aldrich and used without further purification. 5SCB was

dx.doi.org/10.1021/jp4071955 | J. Phys. Chem. B XXXX, XXX, XXX−XXX

synthesized in a two-step procedure starting from 4-bromo-4′-pentylbiphenyl. The aryl bromide was converted to 4-amino-4′-pentylbiphenyl in a reaction analogous to those performed on aryl halides by Lee.[69] The resulting aryl amine was diazotized and reacted with potassium and copper(I) thiocyanates to yield 5SCB.[70,71] The crude brown product was purified with a silica column, yielding a pale-yellow solid. The identity and purity of this solid were verified by ^{1}H and ^{13}C NMR spectroscopy and gas chromatography−mass spectrometry. Details of the synthesis and product characterization are given in the Supporting Information.

For FT-IR and ultrafast infrared experiments, 5CB was sandwiched between two 3 mm CaF_2 windows with a 3.5 μm Mylar spacer (carbon-12 experiments) or 250 μm Teflon spacer (carbon-13 experiments). For 5SCB/5CB mixed sample studies, approximately 2.5 mol % 5SCB was dissolved in 5CB. The solution was then sandwiched between two 3 mm CaF_2 windows with a 250 μm Teflon spacer. In all cases, the spacer thickness was chosen to obtain an FT-IR absorbance of 0.2 to 0.4 for the vibrational probe of interest.

B. FT-IR Spectroscopy. FT-IR experiments were conducted with a Nicolet 6700 FT-IR spectrometer (Thermo Fisher Scientific) with 1 cm^{-1} resolution. The nitrile absorption bands from 5CB are at 2226 and 2174 cm^{-1} for 5^{12}CB and 5^{13}CB, respectively. No background corrections were performed on 5CB spectra, just baseline correction. The CN stretch of 5SCB was found to absorb at 2157 cm^{-1}; a scaled spectrum of 5CB was subtracted as background. FT-IR experiments were performed at temperatures ranging from 298 to 349 K, maintained to ±0.2 K with a PID temperature controller.

C. Ultrafast Infrared Spectroscopy. The experimental setup and methods for the IR pump−probe experiments and 2D IR vibrational echo spectroscopy have been described in detail in previous publications.[17,72] A Ti:Sapphire oscillator and regenerative amplifier pumped an optical parametric amplifier (OPA). The OPA produced ∼6 μJ, ∼120 fs pulses at a 1 kHz repetition rate. The IR center wavelength was tuned to 2225 cm^{-1} (5^{12}CB), 2175 cm^{-1} (5^{13}CB), or 2155 cm^{-1} (5SCB). The mid-IR output of the OPA was split into two or four beams for pump−probe or vibrational echo experiments, respectively. The IR spot sizes at the sample were ∼75 μm.

In the IR pump−probe experiments, a strong pump pulse and a weak probe pulse are crossed in the sample. The polarization-selective pump−probe technique tracks the decay of the probe transmission with polarizations parallel ($I_{\parallel}$) and at the magic angle (I_{ma}, 54.7°) relative to the pump pulse polarization. The data contain information on population relaxation (vibrational lifetime) and, depending on the sample, orientational dynamics:

$$I_{\parallel}(t) = P(t)[1 + 0.8C_2(t)] \quad (1)$$

$$I_{ma}(t) = P(t) \quad (2)$$

where $P(t)$ is the vibrational population relaxation and $C_2(t)$ is the second Legendre polynomial correlation function, which is the transition dipole orientational correlation function for the vibrational mode. Measurement of I_{ma} enables $C_2(t)$ to be extracted from measurements of $I_{\parallel}$ if the orientational relaxation is not too slow. The probe delay relative to the pump was ≤200 ps depending on the sample. The probe (signal) was dispersed by a monochromator acting as a spectrograph and detected by a mercury−cadmium−telluride 32-element array detector. The 1−2 transition portions of the data were analyzed to find vibrational lifetimes, as all of the 0−1 transitions were compromised by heat or by neighboring spectral features as discussed in detail below. Probing the 1−2 transition provides the same lifetime information as probing the 0−1 transition because both decays occur as a result of relaxation from the first vibrationally excited level, 1, to the ground vibrational level, 0. Previously reported OHD-OKE experiments on 5CB showed that at the temperature studied here, 329 K, the exponential complete orientational relaxation occurs in ∼10 ns.[13] On the basis of the vibrational lifetimes of the various vibrational probes, the longest of which is ∼100 ps for 5SCB, a 10 ns orientational relaxation time is not observable with the IR experiments. The OHD-OKE experiments, which measure the derivative of the orientational correlation function (the derivative of the polarizability−polarizability correlation function) also showed that there is limited fast orientation relaxation, which is manifested as a power-law decay in the OHD-OKE experiments.[13,14] However, the correlation function itself decays negligibly on the time scale of the IR pump−probe experiments. In the current experiments, $I_{\parallel}(t)$ and $I_{ma}(t)$ were expected and observed to be the same within experimental error. Therefore, it is sufficient to take the orientational relaxation to be very slow and not contributing to the pump−probe data or the vibrational echo data as discussed below.

In the vibrational echo experiments, three excitation pulses are crossed in the sample. The time between pulses 1 and 2 is the coherence time, τ, and the time between pulses 2 and 3 is the population time, T_w. Nonlinear interactions give rise to a fourth pulse, the vibrational echo, which emerges from the sample in a unique direction at a time $\leq \tau$ after the third excitation pulse. The vibrational echo pulse is overlapped spatially and temporally with an attenuated fourth pulse, which serves as the local oscillator (LO). Interference between the vibrational echo pulse and the LO pulse provides phase information, and heterodyne detection amplifies the vibrational echo. Data were collected by scanning τ at fixed T_w. As τ is scanned, the vibrational echo moves in time relative to the fixed LO, creating a temporal interferogram. The heterodyned vibrational echo, the signal, was frequency-resolved and detected on the array, providing the vertical axis of the 2D IR spectrum, ω_m. The interferograms measured at each ω_m were numerically Fourier transformed to give the horizontal axis of the 2D IR spectrum, ω_τ. A series of 2D IR spectra was collected as a function of T_w.

Information on the structural dynamics of liquid 5CB was obtained from the change in the shape of the 2D IR spectrum as a function of T_w. The time evolution of the shape of the 5^{12}CB or 5^{13}CB band or the CN stretch band of 5SCB reports on spectral diffusion, which occurs because the frequency of the CN stretch changes in response to the structural fluctuations of the medium. A qualitative explanation of the experimental measurement of spectral diffusion is as follows. The CN absorption band is inhomogeneously broadened, that is, there is a range of CN transition frequencies. At a given instant of time, the center frequency of the CN stretch of a particular molecule is determined by the liquid structure in the vicinity of the molecule. The transition frequency of even a single molecule is not a δ function because of homogeneous broadening, which is discussed further below. Homogeneous broadening produces a relatively narrow Lorentzian line shape. The ensemble of all molecules gives the total absorption line, which is a collection of narrow Lorentzians with a Gaussian distribution of center

dx.doi.org/10.1021/jp4071955 | J. Phys. Chem. B XXXX, XXX, XXX−XXX

frequencies. The center frequency of a given molecule is not fixed because the structure of the liquid in a molecule's vicinity evolves in time. The structural evolution causes the frequency of a given molecule's CN stretch to change with time. This is spectral diffusion. On a sufficiently long time scale, all liquid structures occur, and the CN vibration samples all of the frequencies in the inhomogeneously broadened absorption spectrum.

In the vibrational echo pulse sequence, the action of the first and second pulses in effect "labels" the initial vibrational frequencies of the CN vibrational oscillators. In the time between the second and third pulses, T_w, the liquid structure changes, which in turn changes the frequencies of the CN vibrations. The third pulse ends the population time, and the emitted vibrational echo reports on the final frequencies of the CN oscillators. When T_w is very short, little structural evolution occurs, and the readout frequencies are nearly identical to the initially labeled frequencies. As T_w is increased, the environments in the vicinity of the CN oscillators change more and more, and the emission frequencies are increasingly less correlated with their initial frequencies. The loss of correlation is manifested as changes in the shape of the 2D IR spectrum as T_w is increased. At short T_w, the spectrum is elongated along the diagonal, as the detection frequency (ω_m) is approximately the same as the excitation frequency (ω_τ). As the frequencies become less correlated at long T_w, the shape of the spectrum becomes more symmetrical and is completely symmetrical (round) when all of the environments have been sampled. Thus, the rate of liquid structural change in the vicinity of a vibrational probe is manifested in the rate of change in the shape of the 2D IR spectrum.

The frequency−frequency correlation function (FFCF) quantifies the spectral diffusion in terms of the amplitudes and time scales of the dynamics. The FFCF is the joint probability that a vibration with an initial (t = 0) frequency in the inhomogeneous spectral distribution (inhomogeneously broadened vibrational absorption line) will maintain its frequency at a later time t, averaged over all initial frequencies. To extract the FFCF from the T_w dependence of the shape of the 2D IR spectrum, the center-line slope (CLS) method was employed.[73,74] The CLS provides a robust technique for determining the FFCF from the 2D IR data that eliminates many systematic errors.[73,74] In addition, it is a direct observable that can be plotted to illustrate the nature of the time-dependent spectral diffusion dynamics.

The FFCF was modeled with a multiexponential form:

$$C(t) = \langle \delta\omega_{1,0}(\tau_1)\delta\omega_{1,0}(0)\rangle = \sum_i \Delta_i^{\,2} \exp(-t/\tau_i) \quad (3)$$

where Δ_i is the frequency fluctuation amplitude of component i and τ_i is its associated time constant. A component of the FFCF with $\Delta\tau < 1$ is motionally narrowed, and it is a source of the homogeneous broadening of the absorption line. When a component of the dynamics is motionally narrowed, Δ and τ cannot be determined separately. The motionally narrowed homogeneous contribution to the absorption spectrum has a pure dephasing line width given by $\Gamma^* = \Delta^2\tau = 1/\pi T_2^*$, where T_2^* is the pure dephasing time. The observed homogeneous dephasing time, T_2, also has contributions from the vibrational lifetime and orientational relaxation:

$$\frac{1}{T_2} = \frac{1}{T_2^*} + \frac{1}{2T_1} + \frac{1}{3T_{or}} \quad (4)$$

where T_1 and T_{or} are the vibrational lifetime and orientational relaxation time, respectively. The total homogeneous line width is $\Gamma = 1/\pi T_2$. The orientational relaxation time in 5CB is so long (~10 ns) that this term makes a negligible contribution to total homogeneous line width. The vibrational lifetimes of 5^{12}CB and 5^{13}CB are short enough to make non-negligible contributions to the total homogeneous linewidths. The lifetime of the CN stretch of 5SCB is so long that it does not appreciably contribute to the 5SCB homogeneous line width. The CLS, which is determined directly from the 2D IR data, has been shown to be mathematically equivalent to the normalized T_w-dependent portion of the FFCF.[73,74] Combining the CLS data with the linear absorption spectrum permits the determination of the homogeneous contribution, and the process yields the full FFCF.

III. RESULTS AND DISCUSSION

A. ^{12}CN Stretch of 5CB. The ^{12}CN stretch of 5CB (5^{12}CB) gives rise to a fairly narrow peak centered at 2226 cm^{-1}, as shown in Figure 1. (We use 5^{12}CB to indicate the ^{12}CN stretch of 5CB and reserve 5CB for the liquid composed of 5CB nematogens in the isotropic phase.) Although the transition dipoles of nitriles are small, the high concentration of the pure liquid requires the sample to be very thin (3.5 μm) to achieve a reasonable absorbance for nonlinear experiments (i.e., below 0.4). The pump−probe magic-angle decay curve for the 1−2 transition of 5^{12}CB was fit with a single exponential, yielding a vibrational lifetime of 3.6 ± 0.1 ps, which is consistent with previous work on nitriles, where the lifetime ranges from ~1.5 to ~6 ps depending on the particular system.[23,24,54] Pump−probe spectra at several times are shown for 5^{12}CB in Figure 2A. At short time (0.5 ps, black curve), the spectrum consists of a positive-going peak caused by bleaching and stimulated emission of the 0−1 transition and a negative-going peak produced by the new 1−2 absorption resulting from pumping population into the 1 level. By 7 ps (red curve), corresponding to approximately two lifetimes of 5^{12}CB, a new negative-going feature is clearly apparent in the pump−probe spectrum around 2222 cm^{-1}. At 40 ps (blue curve), the negative band for the 1−2 transition is completely gone, demonstrating that there is no

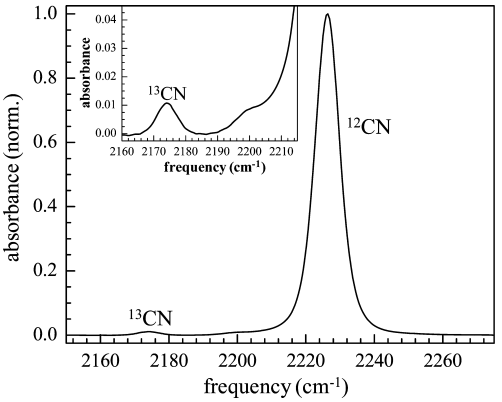

Figure 1. Normalized FT-IR spectrum of the CN stretch of 5CB at 329 K. The ^{12}CN stretch is at 2226 cm^{-1} and is ~8.5 cm^{-1} fwhm. There is a small peak at 2174 cm^{-1} that arises from the natural-abundance ^{13}CN stretch of 5CB. The inset shows an expansion of the ^{13}CN spectral region. The peak ^{13}CN absorbance is ~1% of the ^{12}CN absorbance, in agreement with the 1.1% natural abundance of carbon-13.

dx.doi.org/10.1021/jp4071955 | J. Phys. Chem. B XXXX, XXX, XXX−XXX

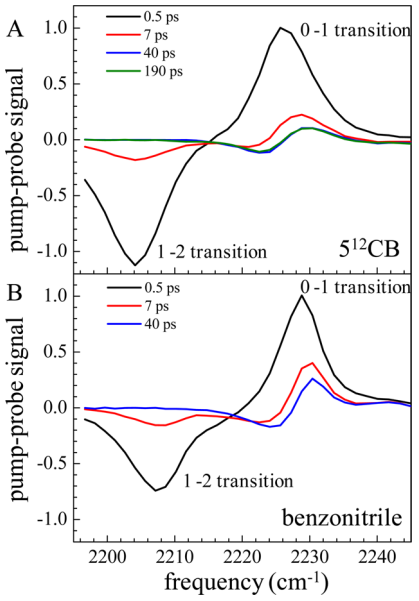

Figure 2. Normalized magic-angle pump−probe spectra of (A) 5^{12}CB and (B) benzonitrile. For both samples, by 7 ps a negative feature is growing in at a frequency ∼3 cm^{-1} lower than that for the 0−1 transition. As the delay increases (40 ps), the spectra are resolved into a residual bleach and new absorption that persist for hundreds of picoseconds, as shown in (A).

longer vibrational excitation. However, the spectrum displays positive- and negative-going peaks of the same size at 2229 and 2222 cm^{-1}, respectively. At 190 ps (green curve), corresponding to ∼50 lifetimes of 5^{12}CB, these features remain unchanged. We attribute the bleach in the ground state and the new absorbance to a shift in the center frequency of 5^{12}CB resulting from heating of the sample. Heat-induced frequency shifts of aromatic nitriles have previously been studied by Kasyanenko et al.[75] in the context of intramolecular vibrational coupling.

The combination of a thin sample, a strong absorption, and the low specific heat of 5CB (∼ 460 J mol^{-1} K^{-1} at 329 K) is conducive to temperature changes of tens of degrees following vibrational relaxation given the amount of energy absorbed by the sample from the pump pulse.[49,76] Temperature-dependent FT-IR measurements carried out on 5CB show a small red shift of 5^{12}CB as the temperature is increased (see Figure S4 in the Supporting Information). This is in agreement with the pump−probe spectra, which display a bleach to the blue side of the initial 5^{12}CB center frequency and a new absorbance on the red side. The persistence of these peaks beyond 200 ps supports our conclusion that sample heating is their source. The heat and the heat-induced long-time pump−probe signal dissipate by thermal diffusion prior to the next pump pulse.

To verify that this heating is not just a feature unique to 5CB, pump−probe experiments were carried out on a sample of benzonitrile. As with 5CB, the high concentration of ^{12}CN in pure benzonitrile required a very thin sample. In this instance, the CaF_2 windows sandwiched benzonitrile without the addition of a spacer to give an absorbance of 0.23. On the basis of the absorbance of the ^{12}CN stretch of benzonitrile with known spacer values, the estimated thickness of this sample was ∼0.8 μm. The pump−probe spectra of the ^{12}CN stretch of benzonitrile at short and long times are shown in Figure 2B. At 0.5 ps (black curve), the spectrum consists of the positive-going 0−1 band and the negative-going 1−2 band. By 7 ps (red curve), the negative-going heating band at 2223 cm^{-1} is apparent. At 40 ps (blue curve), the 1−2 band is gone, showing that there are no vibrational excitations, and the positive and negative heating bands are prominent. These new heating peaks are even more prominent than in 5CB, suggesting greater heating. Even though the benzonitrile sample absorbs less energy from the pump pulse, the thinner sample and lower specific heat (172 J mol^{-1} K^{-1} at 320 K) cause the benzonitrile sample to change temperature drastically as a result of the production of heat by vibrational relaxation following the pump pulse.[77]

The heating observed in the pump−probe spectra of 5^{12}CB is also evident in and causes significant problems in the 2D IR spectra. Figure 3 displays 2D IR spectra of 5^{12}CB at three values

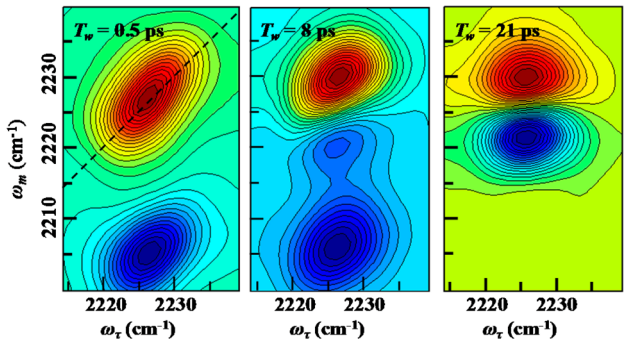

Figure 3. 2D IR spectra of 5^{12}CB at 329 K. At T_w = 0.5 ps (left), a positive 0−1 band (red) and a negative 1−2 band (blue) are present. The dashed line through the 0−1 band is the diagonal. Heating effects are clearly evident at T_w = 8 ps (middle), where a new negative-going absorption appears just below the 0−1 band. At T_w = 21 ps (right), corresponding to ∼6 vibrational lifetimes of 5^{12}CB, the two bands are caused by heat from vibrational relaxation.

of T_w. The very short time spectrum (T_w = 0.5 ps) shows two bands. The red band arises from the 0−1 transition and is positive-going. The blue band arises from vibrational echo emission at the 1−2 transition frequency and is negative-going. The center-to-center frequency difference along the ω_m axis is the vibrational anharmonicity of 5^{12}CB. Consider the 0−1 band. The dashed line in the T_w = 0.5 ps spectrum is the diagonal. At short time, little spectral diffusion has occurred, and the band is substantially elongated along the diagonal. The width perpendicular to the diagonal at short T_w is due to the homogeneous component of the absorption spectrum. At T_w = 0.5 ps, little vibrational relaxation has occurred, and heat has not affected the spectrum. At 8 ps (middle panel), when approximately 90% of the vibrational excitations have relaxed to the ground state and generated heat, a new negative-going peak is evident just below the 0−1 band. At even longer T_w's (e.g., T_w = 21 ps; right panel), the 1−2 transition band has decayed completely, demonstrating that there are no longer vibrational excitations. With no vibrational excitations, there should be no signal. However, two peaks remain. These peaks correspond to the positive-going residual bleach of the ground state and the negative-going new absorbance, both caused by the shifted 5^{12}CB peak center resulting from heating. These bands are the 2D IR manifestation of the long-time heating bands in the pump−probe spectrum in Figure 2A.

The peaks that appear as a result of heating in 5CB impinge upon the 0−1 transition of 5^{12}CB. The presence of these new peaks affects the shape of the 5^{12}CB 2D IR spectra. As the

dx.doi.org/10.1021/jp4071955 | J. Phys. Chem. B XXXX, XXX, XXX−XXX

shapes of the spectra are our source of dynamical information, no reliable information can be gleamed from the 2D IR spectra once they are compromised by the manifestation of heat-induced peaks. Heating effects are obvious when T_w reaches 8 ps, but it is reasonable to assume that they alter the shape of the spectra at earlier times as well. The first appearance of the new negative-going absorbance is at approximately 6 ps, when ~80% of the energy has left the 5^{12}CB vibration. If 6 ps is taken as a maximum window of observation, the CLS decay of the 5^{12}CB band provides limited information on the dynamics of 5CB because of the short range of time that can be observed. Even at 6 ps, the shapes most likely have some heating distortion. The decay can be modeled by a number of functions. As discussed in detail below, spectral diffusion is far from complete at 6 ps.

Heating is not the only concern in a highly concentrated solution. When molecular oscillators are very near each other, there is the possibility of excitation transfer. Simulations of the nematic phase of 5CB suggest that dimers in parallel and antiparallel conformations are present.[61−63] Some of these conformations place the nitrile groups of neighboring molecules in close proximity to each other. Although nitriles have fairly weak transition dipoles, the possibility of excitation transfer still exists. The pseudonematic domains in the isotropic phase of 5CB studied here may also contain configurations of 5CB molecules that place nitriles near each other. Thus, the CLS is conceivably further complicated by excitation transfer from one ^{12}CN to another.

The study of a pure liquid by 2D IR is complicated by heating effects and possible excitation transfer. The problem of excitation transfer is circumvented and heating is reduced in water by studying the OD stretch of dilute HOD in H_2O.[58,59] Experiments on 5CB can also be facilitated by the examination of a low-concentration isotopically labeled probe. The use of a dilute isotopic probe was achieved through the use of natural-abundance ^{13}CN in pure 5CB.

B. ^{13}CN Stretch of 5CB. Closer examination of the main portion of Figure 1 shows a small peak that is red-shifted by ~50 cm^{-1} from the 5^{12}CB vibration. The inset shows an expansion of this spectral region. The small absorption peak is due to the ^{13}CN stretch of 5CB (5^{13}CB; once again, we use 5^{13}CB to indicate the ^{13}CN stretch of 5CB and reserve 5CB for the liquid as a whole). Simple reduced-mass calculations of a nitrile stretch would place the 5^{13}CB vibration at 2179 cm^{-1}. The small shoulder at ~2200 cm^{-1} can be similarly assigned via reduced-mass calculations to a nitrile stretch with the CN containing nitrogen-15. Additionally, the small peak at 2174 cm^{-1} has an absorbance of ~1% of the 5^{12}CB absorbance, which is consistent with the 1.1% natural abundance of carbon-13. Benzonitrile displays a similar shift for the ^{13}CN stretch, with the peak at 2178 cm^{-1} compared with the ^{12}CN stretch at 2230 cm^{-1}.[78] Therefore, we are confident in the assignment of the absorbance at 2174 cm^{-1} to 5^{13}CB.

Because 5^{13}CB is lower in concentration by a factor of ~100 relative to 5^{12}CB, we were able to make samples many times thicker and still have the absorbance of 5^{13}CB remain under 0.4. In the pump−probe and 2D IR experiments we performed, the 5^{13}CB samples were ~70 times thicker than the equivalent 5^{12}CB samples. Because the samples are substantially thicker, laser pulses of the same intensity will heat 5CB by tenths of degrees instead of tens of degrees. Heating of 5CB by less than 1 °C does not cause a significant change in the center frequency of either the 5^{12}CB or 5^{13}CB absorption. Therefore, using 5^{13}CB as a vibrational dynamics probe instead of 5^{12}CB eliminates the heating effects observed when studying pure liquid 5CB. In addition to the mitigation of heating problems, study of 5^{13}CB removes the possibility of excitation transfer because of its low concentration. Therefore, utilizing natural-abundance 5^{13}CB as a probe as opposed to 5^{12}CB in ultrafast IR experiments eliminates both the heating problems and possible excitation transfer that distort the dynamical measurements. Looking at natural-abundance carbon-13 can be considered for the investigation of other pure liquids that have a vibrational probe containing a carbon atom (CO, CH, etc.).

Magic-angle pump−probe experiments on 5^{13}CB were fit with a single exponential, yielding a lifetime of 7.9 ± 0.1 ps. The lifetime was obtained from the 1−2 transition, as the 0−1 transition was obscured by the 1−2 transition of 5^{12}CB. The measured 5^{13}CB lifetime is approximately double that of 5^{12}CB.

To determine whether the extended lifetime of 5^{13}CB relative to 5^{12}CB is a feature unique to 5CB, the vibrational lifetimes of the ^{12}CN and ^{13}CN stretches were measured for benzonitrile. As with 5CB, the benzonitrile ^{13}CN stretch has a longer lifetime than the ^{12}CN stretch (20.2 ± 0.1 vs 5.6 ± 0.1 ps, respectively). Pump−probe decays for the CN stretches of the four species are shown in Figure 4. The large difference in the lifetimes of the ^{13}CN stretches versus the ^{12}CN stretches is evident. In Figure 4, the dashed curves are the single-exponential fits to the pump−probe decays. The increase in lifetime upon isotopic substitution is even more dramatic in benzonitrile than in 5CB.

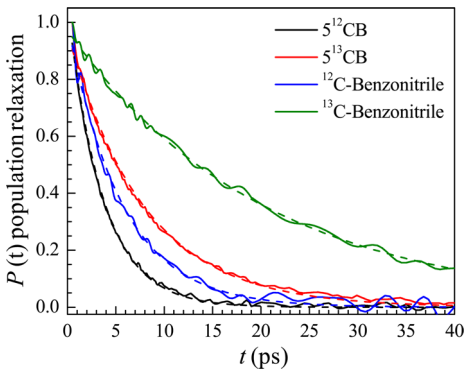

Figure 4. Normalized magic-angle pump−probe decays (solid curves) of 5^{12}CB (2204 cm^{-1}), 5^{13}CB (2154 cm^{-1}), and the ^{12}CN (2207 cm^{-1}) and ^{13}CN (2156 cm^{-1}) stretches of benzonitrile at 329 K. All of the decays are fit well with single-exponential functions (dashed curves). Both 5CB and benzonitrile show an increased vibrational lifetime for the ^{13}CN stretch compared with the ^{12}CN stretch.

The ~50 cm^{-1} shift of the vibrational excitation to lower energy for the carbon-13 species causes a significant increase in the vibrational lifetime. Vibrational relaxation requires the initially excited mode to transfer its energy to a set of lower-frequency modes that conserve energy. The receiving modes can be both intramolecular and intermolecular, and there are many possible pathways.[65] The lowest-order pathway is third-order and requires annihilation of the initially excited CN stretch and the creation of two other modes that have energies that sum to the initial energy. The strongest coupling is generally to intramolecular modes. It is unlikely that there are two intramolecular modes that have energies that sum exactly to the initial CN stretch energy. Therefore, one or more quanta

dx.doi.org/10.1021/jp4071955 | J. Phys. Chem. B XXXX, XXX, XXX−XXX

of the low-frequency continuum of bath modes of the liquid (phonons) are necessary to conserve energy. As the phonons are thermally populated, a phonon can be created or annihilated as needed to conserve energy.[65] For ^{12}CN, the short lifetimes of 5^{12}CB and benzonitrile suggest a low-order process, probably involving the creation of two benzene ring modes and the creation or annihilation of a single phonon of the bath. For the relaxation process to be fast, in addition to strong coupling to intramolecular modes, it is necessary for the phonon mode to be in a region of the phonon dispersion where the density of states is high and the coupling is strong.

The substantial lengthening of the vibrational lifetime of ^{13}CN can arise in a number of ways. First, the 50 cm^{-1} shift to lower energy could change the combination of intramolecular modes that receive the energy. It might be necessary to involve more intramolecular modes, which would be a higher-order (and generally slower) process. It is also possible that the same intramolecular modes are involved but the required bath phonon mode shifts 50 cm^{-1} to lower energy or possibly higher energy if is necessary to annihilate a phonon rather than create one. For non-hydrogen-bonding liquids, the phonon spectrum extends to several hundred wavenumbers. Both 5CB[1] and benzonitrile[79] have bath densities of states with a broad maximum in the range ~20 to ~100 cm^{-1} that extend to ~200 cm^{-1}. If for ^{12}CN the required phonon is near the peak of the density of states (e.g., 60 cm^{-1}) and has good coupling, a shift of 50 cm^{-1} to lower or higher energy would greatly reduce the density of states, and the mechanical nature of the phonon mode will change, which could reduce the coupling.

The extended lifetime of aromatic nitriles upon carbon-13 isotopic substitution of the carbon atom may be useful for ultrafast infrared experiments on peptides and proteins that use the CN stretch of the artificial amino acid cyanophenylalanine as the vibrational dynamics probe. Studies of peptide dynamics have been limited by the short vibrational lifetime of the ^{12}CN stretch.[23,24,29,80] Using ^{13}CN-cyanophenylalanine could substantially increase the range of dynamics that can be measured with 2D IR spectroscopy.

By using 5^{13}CB as the vibrational probe, we eliminated the issues due to heating and possible excitation transfer. Therefore, we were able to acquire 2D IR spectra that accurately depict the dynamics in the pure liquid crystal. The CLS decay obtained for 5^{13}CB extends to waiting times of 28 ps, limited only by the lifetime of the vibration. Figure 5 shows the CLS data (black points) with the fit to a biexponential decay (black curve). The decay time constants are τ_1 = 2.8 ± 0.7 ps and τ_2 = 37 ± 4 ps. As with 5^{12}CB, spectral diffusion is not complete at the end of the experimental window, which is limited by the 7.9 ps vibrational lifetime. Data could be collected to approximately 3.5 lifetimes before the signal became so small as to make the data unreliable. Although the 5^{13}CB experiments allowed us to circumvent the problems observed with 5^{12}CB and greatly extend the time range over which spectral diffusion can be observed, 5^{13}CB does not have a long enough lifetime to monitor the full extent of the structural evolution in 5CB.

C. 5SCB as a Vibrational Probe of 5CB Dynamics. Figure 6 shows an FT-IR spectrum of ~2.5 mol % 5SCB as a solute in 5CB. The CN stretch absorption of 5SCB at 2157 cm^{-1} is comparable in strength to 5^{13}CB. The position and shape of the 5SCB CN stretch peak provide further confirmation of the success of the synthesis, as aromatic thiocyanates have CN stretching mode frequencies around

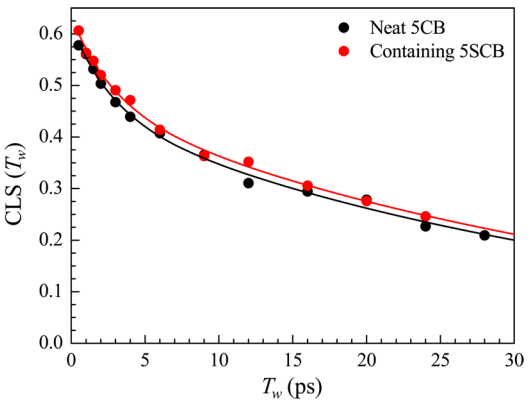

Figure 5. The 2D IR CLS curves for 5^{13}CB in neat 5CB (black) and in 5CB containing 2.5 mol % 5SCB (red). Unlike the 5^{12}CB samples, no significant heating effects are observed in the 2D IR spectra of 5^{13}CB. The acquired CLS data at 329 K are limited only by the vibrational lifetime of the probe. The biexponential fits to these curves are identical within small experimental error, demonstrating that the small amount of 5SCB does not perturb the microscopic properties of the isotropic phase of 5CB.

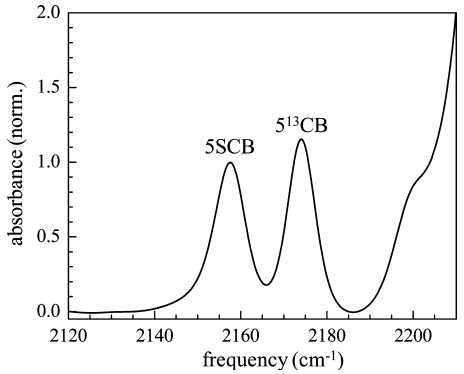

Figure 6. Normalized FT-IR spectrum of 2.5 mol % 5SCB in 5CB with a 250 μm spacer at 329 K. The CN stretch of 5SCB is at 2157 cm^{-1} with ~8.5 cm^{-1} fwhm. Although there is a small amount of overlap of the CN stretch of 5SCB and the 5^{13}CB spectrum, the separation of ~17 cm^{-1} is sufficient for the 2D IR experiments as shown in Figure 7.

2155 cm^{-1} and narrow line shapes.[71,81−84] Because of the low concentration of 5SCB in 5CB, the sample thickness for IR experiments could be increased with negligible heating due to laser excitation and the absence of excitation transfer.

Using the CN stretch of 5SCB as a vibrational probe provides a much longer experimental time window because of its long lifetime. As 5SCB is structurally very similar to 5CB, we anticipated that the dynamics of 5CB would not be significantly perturbed and that the macroscopic properties of the 5CB nematogens in the isotropic phase would not be substantially changed by the addition of a small amount of 5SCB. We conducted detailed temperature-dependent OHD-OKE experiments on samples of 5CB with 2.5 mol % 5SCB in the same manner as in previous studies of nematogens, including 5CB, in the isotropic phase.[13,14] These experiments will be discussed in detail in future work. The mixed sample followed the same Landau−de Gennes temperature dependence of the orientational relaxation as in pure 5CB. The only difference was that the isotropic-to-nematic phase transition temperature is shifted by ~3 K to lower temperature.

dx.doi.org/10.1021/jp4071955 | J. Phys. Chem. B XXXX, XXX, XXX−XXX

To confirm that the microscopic properties of 5CB are relatively unaffected by the addition of 5SCB, 2D IR experiments were performed on 5^{13}CB when 5SCB was present as a solute. Figure 5 shows the CLS curves obtained by monitoring the 5^{13}CB band in neat 5CB (black points) and in 5CB containing 2.5 mol % 5SCB (red points). The curves through the data points are biexponential fits. Within a small experimental error, the 5^{13}CB spectral diffusion with 5SCB present is identical to that of the neat sample. The time constants and amplitudes of the biexponential fits are the same. The sample with 5SCB has a slightly smaller homogeneous line width, which is evidenced by the ~0.03 larger intercept on the ω_m axis. The homogeneous component is caused by ultrafast fluctuations, typically faster than 100 fs. It is not clear whether the difference in the intercepts of the two CLS curves in Figure 5 is real. If it is real, then the addition of 5SCB causes a very small change in the ultrafast structural fluctuations. The experimental window is 25 ps, as determined by the lifetime of the 5^{13}CB vibration. The biexponential fit describes the data well over this limited time window, but as shown below, it does not provide a complete measurement of the dynamics.

Magic-angle pump−probe experiments on the CN stretch of 5SCB showed no evidence of significant heating in the sample. The 1−2 transition of 5^{13}CB obscures the decay of the 0−1 population of the CN stretch of 5SCB; thus, the vibrational lifetime of the CN stretch of 5SCB is taken from its 1−2 population decay. The lifetime of the CN stretch of 5SCB is 103 ± 1 ps. The introduction of the blocking sulfur atom increases the lifetime by factors of ~28 and ~14 relative to 5^{12}CB and 5^{13}CB, respectively. A similar increase has been observed for $C_2H_5CH_2CN$ and $C_2H_5CH_2SCN$ in CCl_4 solution, where the vibrational lifetime increased from 5.5 to 84 ps.[66] The presence of the heavy sulfur atom inhibits vibrational relaxation into the modes of the rest of the molecule, resulting in the large increase in the vibrational lifetime.

While 2D IR experiments on 5^{13}CB were limited by the lifetime of the vibration, experiments on the CN stretch of 5SCB in 5CB are presently limited by the length of our delay lines. 2D spectra were acquired to a waiting time of 180 ps, which is still less than two lifetimes of the vibrational probe. In view of the strength of the signal at 180 ps, it is reasonable to project that it is possible to acquire data to substantially longer times.

Figure 7 shows 2D IR spectra in the spectral region of the CN stretch of 5SCB. At T_w = 0.5 ps (left panel) there are two sets of bands that correspond to the two absorption peaks displayed in Figure 6. The red peaks arise from the 0−1 transitions and are positive-going. Below the positive peaks along the ω_m axis are the negative-going peaks that occur from vibrational echo emission at the 1−2 transition frequency. The difference in the frequencies of the 0−1 and corresponding 1−2 peaks along the ω_m axis is the anharmonic shift caused by the anharmonicity of the vibrational potential. Both sets of peaks are visible at T_w = 0.5 ps because this time is short relative to both lifetimes, 7.9 ps for 5^{13}CB and 103 ps for the CN stretch of 5SCB. The right panel shows the 2D IR spectrum at T_w = 180 ps. Only the CN stretch of 5SCB bands are shown because they are the only bands in the 2D IR spectrum that survive out to this long time. This T_w of 180 ps corresponds to 23 lifetimes for 5^{13}CB, which means the signal is decreased by a factor of 10^{10}, making it undetectable. The change in shape of the CN stretch of 5SCB in the 2D IR spectrum in going from 0.5 to

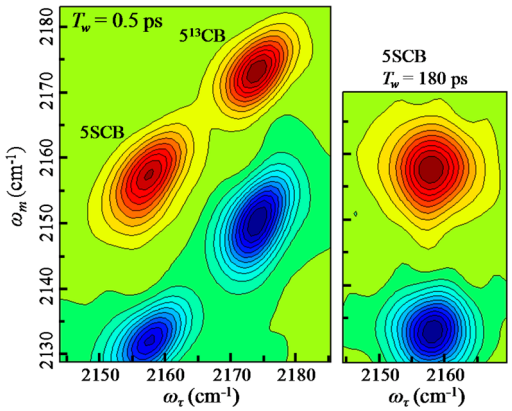

Figure 7. 2D IR spectra of the CN stretch of 2.5 mol % 5SCB in 5CB at 329 K. At T_w = 0.5 ps, 0−1 (red) and 1−2 (blue) transitions are seen for both the CN stretch of 5SCB (lower frequency) and 5^{13}CB (higher frequency). The 5^{13}CB signal decayed completely by ~30 ps because of the short 7.9 ps vibrational lifetime, but the CN stretch transitions of 5SCB are readily detectable at T_w = 180 ps because the CN vibration of 5SCB has a long lifetime of 103 ps.

180 ps is clear, and it provides the basis for the determination of the FFCF.

To ascertain whether the 5SCB probe reports the same structural fluctuations as 5^{13}CB, the early-time CLS data for the CN stretch of 5SCB were compared to those for 5^{13}CB. Figure 8 shows the CLS curves for both species, and the full set of

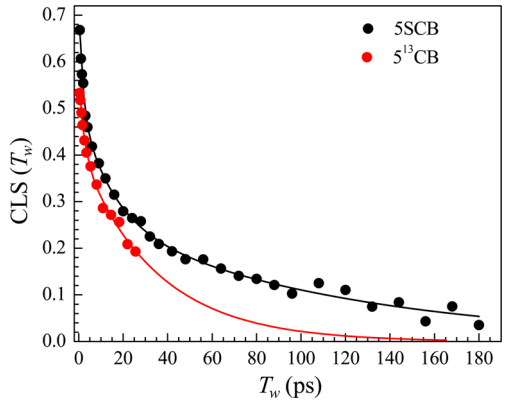

Figure 8. CLS decay curves for the CN stretches of 5SCB in 5CB (black) and 5^{13}CB in 5CB (red). The range of the 5^{13}CB data is limited by the short vibrational lifetime of the ^{13}CN stretch (7.9 ps). Fits to the CN stretch of 5SCB with a biexponential function over the limited time range of the 5^{13}CB data show that the decay constants are the same within experimental error (see Table 1). However, because of the long lifetime of the CN stretch of 5SCB (103 ps), the data can be taken out to much longer times. The full range of the data shows that the decay is actually triexponential with time constants and other FFCF parameters given in Table 1.

FFCF parameters is given in Table 1. The FFCF parameters were obtained using the CLS parameters and the linear absorption spectra.[73,74] The time constants obtained from the CLS are also the FFCF time constants.[73,74] The FFCF gives the true amplitude factors in frequency units rather than unitless normalized amplitudes, and it gives the homogeneous component of the absorption spectrum. When the data for the CN stretch of 5SCB were fit only to the first 25 ps of the CLS decay with a biexponential, which is consistent with the

dx.doi.org/10.1021/jp4071955 | J. Phys. Chem. B XXXX, XXX, XXX−XXX

Table 1. FFCF Parameters

vibrational probe	sample	Δ_1 (cm^{-1})[a]	τ_1 (ps)	Δ_2 (cm^{-1})[a]	τ_2 (ps)	Δ_3 (cm^{-1})[a]	τ_3 (ps)	Γ (cm^{-1})	T_2 (ps)
5^{13}CB	neat 5CB	1.3 ± 0.2	2.8 ± 0.7	2.2 ± 0.2	37 ± 4	–	–	3.1 ± 0.3	3.4 ± 0.3
5^{13}CB	5CB with 5SCB	1.3 ± 0.2	2.8 ± 0.7	2.2 ± 0.2	38 ± 4	–	–	3.0 ± 0.3	3.5 ± 0.3
5SCB, short time	5CB with 5SCB	2.0 ± 0.2	2.0 ± 0.3	2.7 ± 0.2	40 ± 3	–	–	2.5 ± 0.25	4.2 ± 0.4
5SCB, full range	5CB with 5SCB	1.8 ± 0.2	1.6 ± 0.4	1.9 ± 0.2	14 ± 4	2.1 ± 0.2	111 ± 12	2.5 ± 0.25	4.2 ± 0.4
5^{12}CB[b]	neat 5CB	3.0 ± 0.5	9.4 ± 1	–	–	–	–	3.3 ± 0.3	3.3 ± 0.3

[a]The Δ_i are the standard deviations of the i^{th} component of the inhomogeneous contribution to the absorption line. The standard deviation of the total inhomogeneous line width is $(\sum_i \Delta_i^2)^{1/2}$. The full width at half-maximum (fwhm) of the inhomogeneous component of the absorption line is 2.35 times the standard deviation of the total inhomogeneous component. The fwhm of the total absorption spectrum is the convolution of the fwhm of the homogeneous line width, Γ, with the fwhm of the inhomogeneous component. The total absorption line shape is a Voigt profile. [b]As discussed in the text, these data cover a very limited time range and are likely contaminated by heating effects and possibly vibrational excitation transfer.

fitting function used for the available data for 5^{13}CB, the time constants of the decays were the same within experimental error (see rows 2 and 3 of Table 1). The CN stretch of 5SCB has a somewhat smaller homogeneous line width, Γ, and slightly larger inhomogeneous amplitudes, Δ_1 and Δ_2, than 5^{13}CB when both are dilute in 5CB (compare rows 2 and 3 in Table 1), although all of the parameters are almost within the experimental error. There is uncertainty in the 5^{13}CB homogeneous line width Γ (the homogeneous dephasing time T_2) because of problems determining the linear absorption spectrum accurately. We were unable to obtain an accurate line width from the FT-IR spectrum of 5^{13}CB because of the background from the very large neighboring 5^{12}CB peak. While the CLS gives the T_w-dependent parameters, both the CLS and the linear absorption spectrum are necessary to obtain the homogeneous line width. Thus, there is uncertainty in the homogeneous line width, and the difference between the homogeneous line widths of 5^{13}CB and 5SCB may be in part due to experimental error. However, in spite of the uncertainty in the value of the homogeneous line width for 5^{13}CB, it is clear from the CLS data in Figure 8 that at T_w = 0.5 ps the 5SCB line has a smaller homogeneous contribution to the total line than 5^{13}CB. This is seen from the T_w = 0.5 ps values: the 5^{13}CB value is ~0.55 while the 5SCB value is ~0.67. The smaller homogeneous contribution to the total absorption line of 5SCB is actually beneficial, as it permits the observation of the time-dependent structural evolution of a larger fraction of the liquid structures that contribute to the total absorption spectrum. It is clear from these experiments that 5SCB performs well as a probe of the dynamics of 5CB in the isotropic phase. An important point is that the limited time range that can be accessed using 5^{13}CB as the probe does not yield the full picture of the dynamics.

The long lifetime of the 5SCB probe (103 ps) allowed us to examine a much wider experimental time widow that provided a much more complete picture of the dynamics of the 5CB nematogens the isotropic phase. The CLS decay of the CN stretch of 5SCB to 180 ps is shown in Figure 8. Once the greater range of data was available, it became clear that the biexponential fit used for the 5^{13}CB data set, which extends only to 25 ps, is not an adequate description of the dynamics. The full range of data shown in Figure 8 (black points) can be modeled well by a triexponential function. The triexponential fit has time constants of 1.6 ± 0.4, 14 ± 4, and 111 ± 12 ps. The full set of FFCF parameters is given in Table 1, row 4. It is not surprising that CLS data to a T_w of 25 ps were unable to report on a time constant of ~100 ps. The 111 ps component of the true decay caused τ_2 for the slower component of the biexponential fit to the 5^{13}CB data to be too long. Figure 7 shows that the data at 180 ps are still good. As noted above, currently the length of our delay line limits us from going to even longer times. The CLS for the CN stretch of 5SCB at 180 ps has a value of ~0.05 out of 1, and the data shown in Figure 8 are clearly still decaying. Therefore, it is likely that there is not an even slower component. A new delay line with a range to 2 ns will be used subsequently to extend the range of the data.

In an effort to improve our experimental time window even further, we synthesized 4-pentyl-4′-selenocyanobiphenyl (5SeCB), which has an even longer vibrational lifetime due to the heavier selenium atom. (The synthesis will be discussed in future work.) Our preliminary determination of the lifetime is limited by our current delay line, but we estimate a lifetime of 300 to 400 ps. This is again in agreement with an extended lifetime of 282 ps reported for $C_2H_5CH_2SeCN$ in CCl_4.[66] While the use of 5SCB and the current delay line are adequate for the determination of the dynamics at 329 K, as the temperature is lowered toward the isotropic-to-nematic phase transition temperature, ~308 K, the dynamics will slow. The use of 5SeCB and the long delay line will facilitate the examination of the dynamics as the phase transition is approached.

IV. CONCLUDING REMARKS

Pump−probe spectroscopy and 2D IR vibrational echo experiments were conducted to investigate the fast dynamics in the pseudonematic domains of the nematogen 5CB in its isotropic phase. To maintain the liquid-crystal properties of the sample, 5CB must be studied as a pure liquid. The problems associated with studying a pure liquid include drastic heating and possible vibrational excitation transfer. As with experiments to investigate the dynamics of water, we mitigated these problems by employing an isotopically labeled probe. Ultrafast mid-IR studies of water have utilized the OD stretch of a small amount of HOD in H_2O.[28,85−93] Here we have conducted the first 2D IR vibrational echo experiments on a probe containing natural-abundance carbon-13, namely, the natural-abundance ^{13}CN stretch in 5CB. This strategy allowed us to make samples approximately 100 times thicker, eliminating any significant effects from heating in the sample. In addition, the low concentration of 5^{13}CB eliminates the possibility of vibrational excitation transfer. This strategy can be applied to the study of other pure liquids that contain a carbon in the vibrational probe.

We have found that 5^{13}CB has a vibrational lifetime approximately twice that of 5^{12}CB. The increased lifetime of the ^{13}CN stretch is not unique to 5CB; the ^{13}CN stretch of

dx.doi.org/10.1021/jp4071955 | J. Phys. Chem. B XXXX, XXX, XXX−XXX

benzonitrile was found to have an ~4-fold longer vibrational lifetime than the ^{12}CN stretch. The substantial increase in lifetime for both molecules suggests that a different vibrational relaxation pathway occurs because of the approximately 50 cm^{-1} red shift of the ^{13}CN stretch relative to the ^{12}CN stretch. This vibrational pathway could require more intramolecular vibrational modes, different phonon modes of the bath, or both. Increased vibrational lifetime upon carbon-13 substitution in an aromatic nitrile could prove useful in other contexts, such as the study of protein dynamics with ^{13}CN-cyanophenylalanine.

To study the full range of fast dynamics in the isotropic phase of 5CB, we synthesized 5SCB, which was employed as a dilute vibrational probe in 5CB. The sulfur atom between the biphenyl moiety and the nitrile group in 5SCB slows the vibrational relaxation, allowing us to collect 2D IR spectra to ~200 ps. We showed that the microscopic dynamics reported by the CN stretch of 5SCB are essentially the same as those reported by 5^{13}CB over the limited time range of 25 ps over which measurements could be made using the 5^{13}CB probe. However, the measurements out to much longer times using the 5SCB probe demonstrated that the measurements over the shorter time window gave an incomplete and inaccurate picture of the structural dynamics of 5CB. The longer experimental window afforded by 5SCB and the even longer time range that will be possible using 5SeCB will let us study the temperature dependence of the fast dynamics of 5CB as the isotropic-to-nematic phase transition is approached. The influence of pseudonematic domains on an individual probe molecule will be assessed through a comparison to the spectral diffusion of 5SCB in 4-pentylbiphenyl, a molecule that is structurally similar to 5CB but not a nematogen. These measurements will be augmented by temperature-dependent studies of 5CB orientational relaxation dynamics measured with OHD-OKE experiments.[13] A schematic mode coupling theory (MCT) of the OHD-OKE measurements of nematogens in the isotropic phase yields both the orientational correlation function and the density−density correlation function.[14] In a future paper, we will discuss density fluctuations as the apparent cause of spectral diffusion in the liquid crystal 5CB.

■ ASSOCIATED CONTENT

Supporting Information

Synthesis of 4-pentyl-4′-thiocyanobiphenyl, FT-IR spectrum of 5SCB in CCl_4, temperature-dependent FT-IR spectra of 5CB, and NMR spectra. This information is available free of charge via the Internet at http://pubs.acs.org.

■ AUTHOR INFORMATION

Corresponding Author

*E-mail: fayer@stanford.edu.

Notes

The authors declare no competing financial interest.

■ ACKNOWLEDGMENTS

This work was funded by the Division of Chemistry, Directorate of Mathematical and Physical Sciences, National Science Foundation (Grant CHE-1157772).

■ REFERENCES

(1) Hunt, N. T.; Meech, S. R. Orientational and Interaction Induced Dynamics in the Isotropic Phase of a Liquid Crystal: Polarization Resolved Ultrafast Optical Kerr Effect Spectroscopy. *J. Chem. Phys.* **2004**, *120*, 10828−10836.

(2) Pumpa, M.; Cichos, F. Slow Single-Molecule Diffusion in Liquid Crystals. *J. Phys. Chem. B* **2012**, *116*, 14487−14493.

(3) Kim, M. J.; Cardwell, K.; Khitrin, A. K. Nuclear Magnetic Resonance Study of Self-Diffusion in Liquid Crystals. *J. Chem. Phys.* **2004**, *120*, 11327−11329.

(4) Hanson, E. G.; Shen, Y. R.; Wong, G. K. L. Optical-Field-Induced Refractive Indices and Orientational Relaxation Times in a Homologous Series of Isotropic Nematic Substances. *Phys. Rev. A* **1976**, *14*, 1281−1289.

(5) Babkov, L. M.; Gnatyuk, I. I.; Puchkovskaya, G. A.; Trukhachev, S. V. Stucture and Conformational Mobility of 4′-Pentyl-4-Cyanobiphenyl from IR Spectroscopic Data. *J. Struct. Chem.* **2002**, *43*, 1019−1026.

(6) Suzuki, H.; Inaba, A.; Krawczyk, J.; Massalska-Arodz, M.; Kikuchi, T.; Yamamuro, O. Quasi-Elastic Neutron Scattering of Cyanobiphenyl Compounds with Different Terminal Chains. *J. Non-Cryst. Solids* **2011**, *357*, 734−739.

(7) Urban, S.; Gestblom, B.; Dabrowski, R. Comparison of the Dielectric Properties of 4-(2-Methylbutyl)-4′-Cyanobiphenyl (5*CB) and 4-Pentyl-4′-Cyanobiphenyl (5CB) in the Liquid State. *Phys. Chem. Chem. Phys.* **1999**, *1*, 4843−4846.

(8) Gierke, T. D.; Flygare, W. H. Depolarized Rayleigh Scattering in Liquids. Molecular Reorientation and Orientation Pair Correlations in a Nematic Liquid Crystal: MBBA. *J. Chem. Phys.* **1974**, *61*, 2231−2239.

(9) Litster, J. D. Critical Slowing of Fluctuations in a Nematic Liquid Crystal. *J. Appl. Phys.* **1970**, *41*, 996−997.

(10) Stankus, J. J.; Torre, R.; Marshall, C. D.; Greenfield, S. R.; Sengupta, A.; Tokmakoff, A.; Fayer, M. D. Nanosecond Time Scale Dynamics of Pseudo-Nematic Domains in the Isotropic Phase of Liquid Crystals. *Chem. Phys. Lett.* **1992**, *194*, 213−216.

(11) Cang, H.; Li, J.; Fayer, M. D. Short Time Dynamics in the Isotropic Phase of Liquid Crystals: The Aspect Ratio and the Power Law Decay. *Chem. Phys. Lett.* **2002**, *366*, 82−87.

(12) Cang, H.; Li, J.; Novikov, V. N.; Fayer, M. D. Dynamical Signature of Two "Ideal Glass Transitions" in Nematic Liquid Crystals. *J. Chem. Phys.* **2003**, *119*, 10421−10427.

(13) Gottke, S. D.; Cang, H.; Bagchi, B.; Fayer, M. D. Comparison of the Ultrafast to Slow Time Scale Dynamics of Three Liquid Crystals in the Isotropic Phase. *J. Chem. Phys.* **2002**, *116*, 6339−6347.

(14) Li, J.; Cang, H.; Anderson, H. C.; Fayer, M. D. A Mode Coupling Theory Description of the Short and Long-Time Dynamics of Nematogens in the Isotropic Phase. *J. Chem. Phys.* **2006**, *124*, No. 014902.

(15) deGennes, P. G.; Prost, J. *The Physics of Liquid Crystals*; Clarendon Press: Oxford, U.K., 1974.

(16) Cang, H.; Li, J.; Novikov, V. N.; Fayer, M. D. Dynamics in Supercooled Liquids and in the Isotropic Phase of Liquid Crystals: A Comparison. *J. Chem. Phys.* **2003**, *118*, 9303−9311.

(17) Park, S.; Kwak, K.; Fayer, M. D. Ultrafast 2D-IR Vibrational Echo Spectroscopy: A Probe of Molecular Dynamics. *Laser Phys. Lett.* **2007**, *4*, 704−718.

(18) Mukamel, S. *Principles of Nonlinear Optical Spectroscopy*; Oxford University Press: New York, 1995.

(19) Mukamel, S. Multidimensional Femtosecond Correlation Spectroscopies of Electronic and Vibrational Excitations. *Annu. Rev. Phys. Chem.* **2000**, *51*, 691−729.

(20) Asbury, J. B.; Steinel, T.; Stromberg, C.; Corcelli, S. A.; Lawrence, C. P.; Skinner, J. L.; Fayer, M. D. Water Dynamics: Vibrational Echo Correlation Spectroscopy and Comparison to Molecular Dynamics Simulations. *J. Phys. Chem. A* **2004**, *108*, 1107−1119.

(21) Fecko, C. J.; Loparo, J. J.; Roberts, S. T.; Tokmakoff, A. Local Hydrogen Bonding Dynamics and Collective Reorganization in Water: Ultrafast Infrared Spectroscopy of HOD/D_2O. *J. Chem. Phys.* **2005**, *122*, No. 054506.

(22) Cowan, M. L.; Bruner, B. D.; Huse, N.; Dwyer, J. R.; Chugh, B.; Nibbering, E. T. J.; Elsaesser, T.; Miller, R. J. D. Ultrafast Memory Loss and Energy Redistribution in the Hydrogen Bond Network of Liquid H_2O. *Nature* **2005**, *434*, 199−202.

(23) Chung, J. K.; Thielges, M. C.; Bowman, S. J.; Bren, K. L.; Fayer, M. D. Temperature Dependent Equilibrium Native to Unfolded Protein Dynamics and Properties Observed with IR Absorption and 2D IR Vibrational Echo Experiments. *J. Am. Chem. Soc.* **2011**, *133*, 6681−6691.
(24) Chung, J. K.; Thielges, M. C.; Fayer, M. D. Dynamics of the Folded and Unfolded Villin Headpiece (HP35) Measured with Ultrafast 2D IR Vibrational Echo Spectroscopy. *Proc. Natl. Acad. Sci. U.S.A.* **2011**, *108*, 3578−3583.
(25) Finkelstein, I. J.; Zheng, J.; Ishikawa, H.; Kim, S.; Kwak, K.; Fayer, M. D. Probing Dynamics of Complex Molecular Systems with Ultrafast 2D IR Vibrational Echo Spectroscopy. *Phys. Chem. Chem. Phys.* **2007**, *9*, 1533−1549.
(26) Rosenfeld, D. E.; Gengeliczki, Z.; Smith, B. J.; Stack, T. D. P.; Fayer, M. D. Structural Dynamics of a Catalytic Monolayer Probed by Ultrafast 2D IR Vibrational Echoes. *Science* **2011**, *334*, 634−639.
(27) Kim, Y. S.; Hochstrasser, R. M. Applications of 2D IR Spectroscopy to Peptides, Proteins, and Hydrogen-Bond Dynamics. *J. Phys. Chem. B* **2009**, *113*, 8231−8251.
(28) Steinel, T.; Asbury, J. B.; Zheng, J. R.; Fayer, M. D. Watching Hydrogen Bonds Break: A Transient Absorption Study of Water. *J. Phys. Chem. A* **2004**, *108*, 10957−10964.
(29) Chung, J. K.; Thielges, M. C.; Lynch, S. R.; Fayer, M. D. Fast Dynamics of HP35 for Folded and Urea-Unfolded Conditions. *J. Phys. Chem. B* **2012**, *116*, 11024.
(30) Asplund, M. C.; Zanni, M. T.; Hochstrasser, R. M. Two-Dimensional Infrared Spectroscopy of Peptides by Phase-Controlled Femtosecond Vibrational Photon Echoes. *Proc. Natl. Acad. Sci. U.S.A.* **2000**, *97*, 8219−8224.
(31) Mukherjee, P.; Kass, I.; Arkin, I. T.; Zanni, M. T. Picosecond Dynamics of a Membrane Protein Revealed by 2D IR. *Proc. Natl. Acad. Sci. U.S.A.* **2006**, *103*, 3528−3533.
(32) Fang, C.; Hochstrasser, R. M. Two-Dimensional Infrared Spectra of the $^{13}C-^{18}O$ Isotopomers of Alanine Residues in an α-Helix. *J. Phys. Chem. B* **2005**, *109*, 18652−18663.
(33) Kim, Y. S.; Hochstrasser, R. M. Chemical Exchange 2D IR of Hydrogen-Bond Making and Breaking. *Proc. Natl. Acad. Sci. U.S.A.* **2005**, *102*, 11185−11190.
(34) Demirdoven, N.; Cheatum, C. M.; Chung, H. S.; Khalil, M.; Knoester, J.; Tokmakoff, A. Two-Dimensional Infrared Spectroscopy of Antiparallel β-Sheet Secondary Structure. *J. Am. Chem. Soc.* **2004**, *126*, 7981−7990.
(35) Chung, H. S.; Khalil, M.; Tokmakoff, A. Nonlinear Infrared Spectroscopy of Protein Conformational Change During Thermal Unfolding. *J. Phys. Chem. B* **2004**, *108*, 15332−15342.
(36) Demirdoven, N.; Khalil, M.; Golonzka, O.; Tokmakoff, A. Correlation Effects in the Two-Dimensional Vibrational Spectroscopy of Coupled Vibrations. *J. Phys. Chem. A* **2001**, *105*, 8030.
(37) Golonzka, O.; Khalil, M.; Demirdoven, N.; Tokmakoff, A. Vibrational Anharmonicities Revealed by Coherent Two-Dimensional Infrared Spectroscopy. *Phys. Rev. Lett.* **2001**, *86*, 2154−2157.
(38) DeCamp, M. F.; DeFlores, L.; McCracken, J. M.; Tokmakoff, A.; Kwac, K.; Cho, M. Amide I Vibrational Dynamics of *N*-Methylacetamide in Polar Solvents: The Role of Electrostatic Interactions. *J. Phys. Chem. B* **2005**, *109*, 11016−11026.
(39) Eaves, J. D.; Loparo, J. J.; Fecko, C. J.; Roberts, S. T.; Tokmakoff, A.; Geissler, P. L. Hydrogen Bonds in Liquid Water Are Broken Only Fleetingly. *Proc. Natl. Acad. Sci. U.S.A.* **2005**, *102*, 13019−13022.
(40) Eaves, J. D.; Tokmakoff, A.; Geissler, P. L. Electric Field Fluctuations Drive Vibrational Dephasing in Water. *J. Phys. Chem. A* **2005**, *109*, 9424−9436.
(41) Fecko, C. J.; Eaves, J. D.; Loparo, J. J.; Tokmakoff, A.; Geissler, P. L. Ultrafast Hydrogen-Bond Dynamics in the Infrared Spectroscopy of Water. *Science* **2003**, *301*, 1698−1702.
(42) Loparo, J. J.; Fecko, C. J.; Eaves, J. D.; Roberts, S. T.; Tokmakoff, A. Reorientational and Configurational Fluctuations in Water Observed on Molecular Length Scales. *Phys. Rev. B* **2004**, *70*, No. 180201.
(43) Loparo, J. J.; Roberts, S. T.; Tokmakoff, A. Multidimensional Infrared Spectroscopy of Water. I. Vibrational Dynamics in Two-Dimensional IR Line Shapes. *J. Chem. Phys.* **2006**, *125*, No. 194521.
(44) Loparo, J. J.; Roberts, S. T.; Tokmakoff, A. Multidimensional Infrared Spectroscopy of Water. II. Hydrogen Bond Switching Dynamics. *J. Chem. Phys.* **2006**, *125*, No. 194522.
(45) Dong, R. Y. Modeling of Dynamics in Liquid Crystals from Deuterium NMR. *J. Chem. Phys.* **1988**, *88*, 3962−3969.
(46) Ghanadzadeh, A.; Beevers, M. S. Dielectric Investigations and Molecular Association in Non-Mesogenic and Mesogenic Solutions. *J. Mol. Liq.* **2002**, *102*, 365−377.
(47) Gray, G. W.; Harrison, K. J.; Nash, J. A. New Family of Nematic Liquid Crystals for Displays. *Electron. Lett.* **1973**, *9*, 130−131.
(48) Horn, R. G. Refractive Indices and Order Parameters of Two Liquid Crystals. *J. Phys.* **1978**, *39*, 105−109.
(49) Iannacchione, G. S.; Finotello, D. Calorimetric Study of Phase Transitions in Confined Liquid Crystals. *Phys. Rev. Lett.* **1992**, *69*, 2094−2097.
(50) Jadzyn, J.; Czechowski, G. Pre-Transitional Temperature Behavior of the Shear Viscosity of Freely Flowing Thermotropic Liquid Crystals. *Phase Transitions* **2007**, *80*, 665−673.
(51) Kang, D. S.; Kwon, K.-s.; Kim, S. I.; Gong, M.-s.; Seo, S. S. A.; Noh, T. W.; Joo, S.-w. Temperature-Dependent Raman Spectroscopic Study of the Nematic Liquid Crystal 4-*N*-Pentyl-4′-Cyanobiphenyl. *Appl. Spectrosc.* **2005**, *59*, 1136−1140.
(52) Li, J.; Wang, I.; Fayer, M. D. Ultrafast to Slow Orientational Dynamics of a Homeotropically Aligned Nematic Liquid Crystal. *J. Phys. Chem. B* **2005**, *109*, 6514−6519.
(53) Kobayashi, T.; Yoshida, H.; Chandani, A. D. L.; Kobinata, S.; Maedea, S. Molecular Ordering in Liquid Crystals and the Effect of End-Chains on the Even−Odd Effect. *Mol. Cryst. Liq. Cryst.* **1986**, *136*, 267−279.
(54) Bagchi, S.; Boxer, S. G.; Fayer, M. D. Ribonuclease S Dynamics Measured Using a Nitrile Label with 2D IR Vibrational Echo Spectroscopy. *J. Phys. Chem. B* **2012**, *116*, 4034−4042.
(55) Kropman, M. F.; Nienhuys, H.-K.; Woutersen, S.; Bakker, H. J. Vibrational Relaxation and Hydrogen-Bond Dynamics of HDO:H_2O. *J. Phys. Chem. A* **2001**, *105*, 4622−4626.
(56) Rezus, Y. L. A.; Bakker, H. J. Orientational Dynamics of Isotopically Diluted H_2O and D_2O. *J. Chem. Phys.* **2006**, *125*, No. 144512.
(57) Asbury, J. B.; Steinel, T.; Kwak, K.; Corcelli, S. A.; Lawrence, C. P.; Skinner, J. L.; Fayer, M. D. Dynamics of Water Probed with Vibrational Echo Correlation Spectroscopy. *J. Chem. Phys.* **2004**, *121*, 12431−12446.
(58) Woutersen, S.; Bakker, H. J. Resonant Intermolecular Transfer of Vibrational Energy in Liquid Water. *Nature* **1999**, *402*, 507−509.
(59) Gaffney, K. J.; Piletic, I. R.; Fayer, M. D. Orientational Relaxation and Vibrational Excitation Transfer in Methanol−Carbon Tetrachloride Solutions. *J. Chem. Phys.* **2003**, *118*, 2270−2278.
(60) Rosenfeld, D. E.; Fayer, M. D. Excitation Transfer Induced Spectral Diffusion and the Influence of Structural Spectral Diffusion. *J. Chem. Phys.* **2012**, *137*, No. 064109.
(61) Wilson, M. R.; Dunmur, D. A. Molecular Mechanics Modelling of Structure/Property Relationships in Liquid Crystals. *Liq. Cryst.* **1989**, *5*, 987−999.
(62) Amovilli, C.; Cacelli, I.; Campanile, S.; Prampolini, G. Calculation of the Intermolecular Energy of Large Molecules by a Fragmentation Scheme: Application to the 4-*N*-Pentyl-4′-Cyanobiphenyl (5CB) Dimer. *J. Chem. Phys.* **2002**, *117*, 3003−3012.
(63) Zhang, J.; Su, J.; Guo, H. An Atomistic Simulation for 4-Cyano-4′-Pentylbiphenyl and Its Homologue with a Reoptimized Force Field. *J. Phys. Chem. B* **2011**, *115*, 2214−2227.
(64) Tokmakoff, A.; Sauter, B.; Fayer, M. D. Temperature-Dependent Vibrational Relaxation in Polyatomic Liquids: Picosecond Infrared Pump−Probe Experiments. *J. Chem. Phys.* **1994**, *100*, 9035−9043.

(65) Kenkre, V. M.; Tokmakoff, A.; Fayer, M. D. Theory of Vibrational Relaxation of Polyatomic Molecules in Liquids. *J. Chem. Phys.* **1994**, *101*, 10618−10629.
(66) Bian, H.; Li, J.; Wen, X.; Zheng, J. Mode-Specific Intermolecular Vibrational Energy Transfer. I. Phenyl Selenocyanate and Deuterated Chloroform Mixture. *J. Chem. Phys.* **2010**, *132*, No. 184505.
(67) Bian, H.; Wen, X.; Li, J.; Zheng, J. Mode-Specific Intermolecular Vibrational Energy Transfer. II. Deuterated Water and Potassium Selenocyanate Mixture. *J. Chem. Phys.* **2010**, *133*, No. 034505.
(68) Li, J.; Bian, H.; Chen, H.; Wen, X.; Hoang, B. T.; Zheng, J. Ion Association in Aqueous Solutions Probed through Vibrational Energy Transfers among Cation, Anion and Water Molecules. *J. Phys. Chem. B* **2013**, *117*, 4274−4283.
(69) Lee, S.; Jorgensen, M.; Hartwig, J. F. Palladium-Catalyzed Synthesis of Arylamies from Aryl Halides and Lithium Bis-(trimethylsilyl)amide as an Ammonia Equivalent. *Org. Lett.* **2001**, *3*, 2729−2732.
(70) Hansch, C.; Schmidhalter, B.; Reiter, F.; Saltonstall, W. Catalytic Synthesis of Heterocycles. VIII. Dehydrocyclization of *o*-Ethylbenzenethiols to Thianaphenes. *J. Org. Chem.* **1956**, *21*, 265−270.
(71) Ciszek, J. W.; Stewart, M. P.; Tour, J. M. Spontaneous Assembly of Organic Thiocyanates on Gold Surfaces. Alternative Precursors for Gold Thiolate Assemblies. *J. Am. Chem. Soc.* **2004**, *126*, 13172−13173.
(72) Zheng, J.; Kwak, K.; Fayer, M. D. Ultrafast 2D IR Vibrational Echo Spectroscopy. *Acc. Chem. Res.* **2007**, *40*, 75−83.
(73) Kwak, K.; Park, S.; Finkelstein, I. J.; Fayer, M. D. Frequency−Frequency Correlation Functions and Apodization in 2D-IR Vibrational Echo Spectroscopy, a New Approach. *J. Chem. Phys.* **2007**, *127*, No. 124503.
(74) Kwak, K.; Rosenfeld, D. E.; Fayer, M. D. Taking Apart the Two-Dimensional Infrared Vibrational Echo Spectra: More Information and Elimination of Distortions. *J. Chem. Phys.* **2008**, *128*, No. 204505.
(75) Kasyanenko, V. M.; Keiffer, P.; Robtsov, I. V. Intramolecular Vibrational Coupling Contribution to Temperature Dependence of Vibrational Mode Frequencies. *J. Chem. Phys.* **2012**, *136*, No. 144503.
(76) Finotello, D.; Iannacchione, G. S. High Resolution Calorimetric Studies at Phase Transitions of Alkylcyanobiphenyl Liquid Crystals Confined to Submicron Size Cylindrical Cavities. *Int. J. Mod. Phys. B* **1995**, *9*, 109−145.
(77) Lei, Y.; Chen, Z.; An, X.; Huang, M.; Shen, W. Measurements of Density and Heat Capacity of Binary Mixtures {*X* Benzonitrile + (1 − *X*)(Octane or Nonane)}. *J. Chem. Eng. Data* **2010**, *55*, 4154−4161.
(78) Bak, B.; Nielsen, J. T.; Lipschitz, L. Preparation of Benzonitrile, Isotopically Labelled in the Cyanide Group. *Acta Chem. Scand.* **1961**, *15*, 949.
(79) Smith, N. A.; Meech, S. R. Optically-Heterodyne-Detected Optical Kerr Effect (OHD-OKE): Applications in Condensed Phase Dynamics. *Int. Rev. Phys. Chem.* **2002**, *21*, 75−100.
(80) Urbanek, D. C.; Vorobyev, D. Y.; Serrano, A. L.; Gai, F.; Hochstrasser, R. M. The Two-Dimensional Vibrational Echo of a Nitrile Probe of the Villin HP35 Protein. *J. Phys. Chem. Lett.* **2010**, *1*, 3311−3315.
(81) Clark, J. H.; Jones, C. W.; Duke, C. V. A.; Miller, J. M. Aromatic Thiocyanation Using Supported Copper (I) Thiocyanate. *J. Chem. Soc., Chem. Commun.* **1989**, 81−82.
(82) Bailey, A. L.; Bates, G. S. Synthesis of Isocyano and (Haloalkynyl)Biphenyls: New Thermotropic Liquid Crystals. *Mol. Cryst. Liq. Cryst.* **1991**, *198*, 417−428.
(83) Challenger, F.; Peters, A. T. The Nitration of Aromatic Thiocyanates and Selenocyanates. *J. Chem. Soc.* **1928**, 1364−1375.
(84) Fafarman, A. T.; Webb, L. J.; Chuang, J. I.; Boxer, S. G. Site-Specific Conversion of Cysteine Thiols into Thiocyanate Creates an IR Probe for Electric Fields in Proteins. *J. Am. Chem. Soc.* **2006**, *128*, 13356−13357.
(85) Giammanco, C. H.; Wong, D. B.; Fayer, M. D. Water Dynamics in Divalent and Monovalent Concentrated Salt Solutions. *J. Phys. Chem. B* **2012**, *116*, 13781−13792.
(86) Moilanen, D. E.; Piletic, I. R.; Fayer, M. D. Tracking Water's Response to Structural Changes in Nafion Membranes. *J. Phys. Chem. A* **2006**, *110*, 9084−9088.
(87) Zheng, J. R.; Kwak, K.; Chen, X.; Asbury, J. B.; Fayer, M. D. Formation and Dissociation of Intra-Intermolecular Hydrogen-Bonded Solute−Solvent Complexes: Chemical Exchange Two-Dimensional Infrared Vibrational Echo Spectroscopy. *J. Am. Chem. Soc.* **2006**, *128*, 2977−2987.
(88) Moilanen, D. E.; Levinger, N.; Spry, D. B.; Fayer, M. D. Confinement or the Nature of the Interface? Dynamics of Nanoscopic Water in Reverse Micelles. *J. Am. Chem. Soc.* **2007**, *129*, 14311−14318.
(89) Park, S.; Fayer, M. D. Hydrogen Bond Dynamics in Aqueous NaBr Solutions. *Proc. Natl. Acad. Sci. U.S.A.* **2007**, *104*, 16731−16738.
(90) Zheng, J. R.; Fayer, M. D. Hydrogen Bond Lifetimes and Energetics for Solute/Solvent Complexes Studied with 2D-IR Vibrational Echo Spectroscopy. *J. Am. Chem. Soc.* **2007**, *129*, 4328−4335.
(91) Fenn, E. E.; Wong, D. B.; Fayer, M. D. Water Dynamics at Neutral and Ionic Interfaces. *Proc. Natl. Acad. Sci. U.S.A.* **2009**, *106*, 15243−15248.
(92) Fenn, E. E.; Wong, D. B.; Fayer, M. D. Water Dynamics in Small Reverse Micelles in Two Solvents: Two-Dimensional Infrared Vibrational Echoes with Two-Dimensional Background Subtraction. *J. Chem. Phys.* **2011**, *134*, No. 054512.
(93) Yang, M.; Li, F.; Skinner, J. L. Vibrational Energy Transfer and Anisotropy Decay in Liquid Water: Is the Forster Model Valid? *J. Chem. Phys.* **2011**, *135*, No. 164505.